Interplay between membrane tension and the actin cytoskeleton determines shape changes

Camille Chane Simon, Valentina Caorsi, Clément Campillo, C. Sykes

Physical Biology

OFFICIAL JOURNAL OF
Sociedad de Biofísicos Latino Americanos

PAPER • OPEN ACCESS

Interplay between membrane tension and the actin cytoskeleton determines shape changes

To cite this article: Camille Simon *et al* 2018 *Phys. Biol.* **15** 065004

IOP Publishing Phys. Biol. 15 (2018) 065004 https://doi.org/10.1088/1478-3975/aad1ab

Physical Biology

OPEN ACCESS

RECEIVED
9 February 2018

REVISED
3 July 2018

ACCEPTED FOR PUBLICATION
6 July 2018

PUBLISHED
27 July 2018

PAPER

Interplay between membrane tension and the actin cytoskeleton determines shape changes

Camille Simon[1,2], Valentina Caorsi[1,2], Clément Campillo[3] and Cécile Sykes[1,2,4]

[1] Laboratoire Physico Chimie Curie, Institut Curie, PSL Research University, CNRS UMR168, 75005, Paris, France
[2] Sorbonne Universités, UPMC Univ Paris 06, 75005, Paris, France
[3] LAMBE, Université Evry Val d'Essonne, CNRS, CEA, Université Paris-Saclay, Evry F-91025, France
[4] Author to whom any correspondence should be addressed.

E-mail: cecile.sykes@curie.fr

Keywords: actin dynamics, membrane, deformation, capping protein

Supplementary material for this article is available online

Abstract

The ability of mammalian cells to deform their membrane relies on the action of the cytoskeleton. In particular, the dynamics of the actin cytoskeleton, assembling at the plasma membrane, plays a crucial role in controlling cell shape. Many proteins are involved to ensure proper growth of the actin network at the cell membrane. The detailed structure of this network regulates the force that is necessary for membrane deformation. We address here how the presence of capping proteins, which limit the length of actin filaments and thus affects network topology, influences membrane shape. We use a system of liposomes, activated to polymerize actin at their surface, and placed in a mixture of purified proteins that reconstitutes actin dynamics. Our system also allows the variation of membrane tension by deflating the liposomes. We show that membrane deformations are clearly favored in the presence of capping proteins in the actin network. Moreover, in the absence of capping proteins, membrane deformations appear only when the liposomes are deflated. Our results unveil that the interplay between membrane tension and actin network structure and dynamics governs cell shape.

Introduction

Changes in shape are crucial for mammalian cells to accomplish their vital functions such as motility, trafficking, or division. These functions are achieved through deformations of the cell membrane into either protrusions, such as lamellipodia, filopodia, or invaginations, such as endocytosis, or into a global shape change such as a dumbbell-shape or an elongated one in the case of division. Such structures are essentially based on a polymerizing actin cytoskeleton growing underneath the plasma membrane [1, 2]. This actin network can arrange in different organizations (parallel bundles, branched network) to drive cell shape changes [3].

The mechanism of force production based on actin dynamics was first studied by observing intracellular parasites that hijack the actin machinery for their own propulsion. The movement of *Listeria monocytogenes* is indeed based on the dynamic assembly of an actin network activated at its surface [4, 5]. Beads coated with an activator of actin polymerization mimic this actin-based movement and move within cell extracts or purified proteins, propelled by the same 'actin tail' that propels *Listeria* [6, 7]. In particular, a branched actin network, generated by the Arp2/3 complex, is able to create mechanical stresses that build up during the growth of the actin network. At the bead surface, these stresses operate perpendicularly to the surface whereas further at the external edge of the network, they are tangential [8]. Such a stress buildup results in a breakage of the actin network (called 'symmetry breaking'), as soon as the tangential stress at the edge of the network exceeds a threshold value that is sufficient to break a bond in the network and initiate a fracture [9]. As a consequence, unbalanced forces following symmetry breaking lead to the onset of actin-based propulsion [6, 9, 10]. Propulsion of hard objects based on actin polymerization involves mechanical deformations within the actin network over a distance that is about twice the size of the object, as evidenced by photobleaching the actin network [11]. Such deformations are the signature of stresses within the actin network,

that can be transmitted to the object and lead to its propulsion and compression.

When oil droplets or liposomes are used instead of beads or bacteria (which have a hard wall and therefore are not deformable), the same mechanisms are at work except that, this time, the surface is deformable and fluid. Symmetry breaking of the actin network occurs, oil droplets and liposomes undergo actin-based motility [12–14]. They are deformed into a pear or a symmetrical elongated kiwi shape depending on the attachment strength of the network to the surface (for a review see [15]). This propulsion is accompanied by a convective movement of the activators of actin polymerization on the membrane [16, 17]. Deformations of liposomes can lead to vesicle pinch off under the sole effect of actin polymerization [18].

Changing the mechanical properties of the actin network, through modifying the composition of the protein mixture, affects the propulsion velocity of beads and time for symmetry breaking, leading generally to bell-shaped curves as a function of protein concentrations [9]. With the Arp2/3 complex promoting the formation of new branches at the liposome surface and capping proteins tuning filament length, there is a way of modulating the detailed network topology through the relative concentrations of both proteins. Indeed, as already shown on beads and liposomes, the concentration of capping proteins, relatively to the one of the Arp2/3 complex, modulates the actin network architecture, such as the network mesh size and entanglement, quantified in [19]. However, little is known about the role of the detailed actin structure, or of membrane tension on liposome shape changes. In fact, actin polymerization and membrane tension forces may play against each other. Here, we characterize how liposomes deform during symmetry breaking, and address how this phenomenon depends on the organization of the actin network, and on membrane tension. These parameters can be perfectly controlled in a reconstituted system of liposomes placed in an actin mix that promotes actin polymerization. We generate liposomes at the surface of which a dynamic branched actin network grows from the assembly of purified proteins. We show that symmetry breaking of the actin network is correlated with liposome deformability and depends on network composition and membrane tension.

Methods

Reagents, lipids, proteins

Chemicals are purchased from Sigma Aldrich (St. Louis, MO, USA) unless specified otherwise. L-alpha-phosphatidylcholine (EPC) and 1,2-distearoyl-sn-glycero-3-phosphoethanolamine-N-[biotinyl polyethylene glycol 2000] (biotinylated lipids) are purchased from Avanti polar lipids (Alabaster, USA). Texas Red® 1,2-dipalmitoyl-sn-glycero-3-phosphocholine, triethylammonium salt is from Thermofisher (Walthham, USA). Actin is purchased from Cytoskeleton (Denver, USA) and used with no further purification. Fluorescent Alexa-488 actin is obtained from Molecular Probes (Eugene, Oregon, USA). Porcine Arp2/3 complex is purchased from Cytoskeleton and used with no further purification. Mouse $\alpha 1\beta 2$ capping protein is purified as in [20]. Untagged human profilin and SpVCA are purified as in [21]. A solution of 30 μM monomeric actin containing 15% of labelled Alexa-488 actin is obtained by incubating the actin solution in G-Buffer (2 mM Tris, 0.2 mM CaCl2, 0.2 mM DTT, pH 8.0) overnight at 4 °C. All proteins (SpVCA, profilin, capping protein, actin) are mixed in the isotonic or hypertonic working buffer. The isotonic working buffer contains 25 mM imidazole, 70 mM sucrose, 1 mM Tris, 50 mM KCl, 2 mM MgCl2, 0.1 mM DTT, 1.6 mM ATP, 0.02 mg $\cdot$ mL^{-1} β-casein, adjusted to pH 7.4. The hypertonic working buffer differs only by its sucrose concentration and contains 25 mM imidazole, 320 mM sucrose, 1 mM Tris, 50 mM KCl, 2 mM MgCl2, 0.1 mM DTT, 1.6 mM ATP, 0.02 mg mL^{-1} β-casein, adjusted to pH 7.4. Osmolarities of the isotonic and hypertonic working buffers are respectively 200 and 400 mOsmol, as measured with a vapor pressure osmometer (VAPRO 5600).

Liposome preparation

Liposomes are prepared using the electroformation technique [22]. Briefly, 10 μL of a mixture of EPC lipids, 0.1% biotinylated lipids and 0.1% TexasRed lipids with a concentration of 2.5 mg $\cdot$ mL^{-1} in chloroform/methanol 5:3 (v/v) are spread onto indium tin oxide (ITO)-coated plates and placed under vacuum for 2 h. A chamber is formed using the ITO plates (their conductive sides facing each other) filled with a sucrose buffer (0.2 M sucrose, 2 mM Tris adjusted at pH 7.4) and sealed with hematocrit paste (Vitrex Medical, Denmark). Liposomes are formed by applying an alternate current voltage (10 Hz, 1 V rms) for 2 h. Liposomes are then incubated with an activator of actin polymerization (S-pVCA, 350 nM) for 15 min. Liposomes ('non-deflated') are used right away for polymerizing actin in the isotonic working buffer. For 'deflated' liposomes, an extra step is added, as they are diluted twice in the hypertonic working buffer at 400 mOsmol and incubated for 30 min. The final solution is therefore at 300 mOsmol.

Actin cortices with a branched network

Actin polymerization is triggered by diluting the non-deflated or deflated liposomes 6 times in a mix of respectively isotonic or hypertonic working buffer containing final concentrations of 3 μM monomeric actin (15% fluorescently labelled with AlexaFluor488), 3 μM profilin, 37 nM Arp2/3 complex, 25 nM capping protein. Note that the final concentrations of salt and ATP in both isotonic and hypertonic conditions are 0.3 mM NaCl, 41 mM KCl, 1.6 mM $MgCl_2$, 0.02 mM $CaCl_2$ and 1.5 mM ATP. Hypertonic conditions only

differ from isotonic conditions by 250 mM sucrose. To be able to keep the same actin activity in non-deflated or deflated conditions, one point of attention is that reagent concentrations for actin polymerization must be unchanged in concentration, as noted above for both conditions. Therefore we can investigate the exclusive role of membrane tension, independently of actin dynamics.

Observation of liposomes

Observation in 2D: epifluorescence (GFP filter cube, excitation 470 nm, emission 525 nm; Texas red filter cube: excitation 545–580 nm, emission 610 nm-IR), phase contrast and bright-field microscopy are performed using an IX70 Olympus inverted microscope with a 100× or a 60× oil-immersion objective. Images are collected by a charge coupled device CCD camera (CoolSnap, Photometrics, Roper Scientific).

Image analysis

Image analyses are performed with FIJI software and data are processed on Matlab and Excel.

Characterization of membrane deformations

Liposome contour is detected from membrane fluorescence images either using the *Wand tool* on FIJI software or detected manually. Liposome shape is then characterized by its elliptical form factor (latter named 'form factor') $e = \frac{b}{a}$ where b and a are respectively the minor and the major axis of the ellipse best fitting the liposome contour (same area, orientation and centroid as the original selection, FIJI software).

Analysis of the symmetry breaking of the actin network

To characterize the anisotropy of the actin network representative of a symmetry breaking event, we first detect the contour of the liposome on fluorescent membrane images (see above). We next record the actin fluorescence profile (I is the fluorescence intensity) along this contour on a 30 pixel width and obtain I_{max} and I_{min} as respectively the maximum and minimum of the fluorescence intensity over the contour length. We define $\text{Asym} = \frac{I_{max} - I_{min}}{I_{max}}$. Then, we proceed in two steps using images (a) and (b) of figure S1 as references for an unambiguous symmetry breaking event.

- For $\text{Asym} > 0.5$, we state that there is an asymmetry in the actin network that may reveal a symmetry breaking event (figure S1(a)–(d)) that will be further analyzed by the width of the fluorescence distribution (see below). Then, raw intensity profiles, plotted as a normalized intensity $\frac{I - I_{min}}{I_{max} - I_{min}}$ as a function of the normalized contour length, are smoothed by a moving average filter of span 5 ('smooth' function on Matlab, and figure S1).
  - Cases where profiles have more than one peak that crosses the half-height (normalized intensity =0.5) are considered as non-symmetry breaking events because the actin is not distributed only one side.
  - For other profiles, we measure the width at half-height, w, and we set a threshold of $w = 0.25$ for a true symmetry breaking event (evaluated from figure S1, images (a) and (b)).
- If $\text{Asym} \leqslant 0.5$, we conclude that the actin network does not break the symmetry (figure S1, images (e) and (f)).

Results

Observation of the actin network symmetry breaking around cell-sized liposomes

In order to observe the symmetry breaking of an actin network, based on what was observed around hard spheres [19], a dynamic, branched, Arp2/3-based, actin network is reconstituted at the outer surface of electroformed liposomes (Methods). The Arp2/3 complex is activated at the membrane surface through the use of a fragment of WASP (the Wiskott–Aldrich syndrome protein), pVCA, tagged with a streptavidin, hereafter named SpVCA. This protein SpVCA is grafted to the biotinylated lipids of the liposomes through its streptavidin tag (Methods and figure 1(a)). Liposomes, once coated with SpVCA, are then placed in a mixture containing monomeric actin, profilin, the Arp2/3 complex and capping proteins (CP) (figure 1(a), left). As already reported, the presence of CP in the actin polymerization mixture allows to break the symmetry of the actin network within a few to tens of minutes, depending on liposome size [21, 23]. Indeed, the actin network grows by forming new branches at the liposome surface, therefore putting the network under tension, especially at the outer layer, until a critical stress is reached, and the actin shell breaks open [9]. We observe liposomes after 60 min of incubation in the actin mix. Whereas they are mainly spherical initially, at 60 min, they appear highly deformed by the symmetry breaking event into a pear or dumbbell (figure 1(c), top row). Symmetry breaking of the actin network is defined as the presence of an asymmetric actin network around the liposome (Methods). Such a symmetry breaking event is spontaneous, and is generally followed by directional actin-based motion with the growth of a propelling, growing actin 'comet-tail', as it was called for the propulsion of bacteria such as *Listeria* [4, 24] or of beads mimicking *Listeria* [7, 6]. We indeed observe such comet tails, as illustrated in supplementary figures S1(a) and (b) (stacks.iop.org/PhysBio/15/065004/mmedia). In order to define the symmetry breaking event in a quantitative way, we use the fluorescence images and define a threshold of asymmetry of the fluorescence of actin along the membrane contour (Methods and figure S1). We find that in the presence of CP, 47.3% of liposomes display

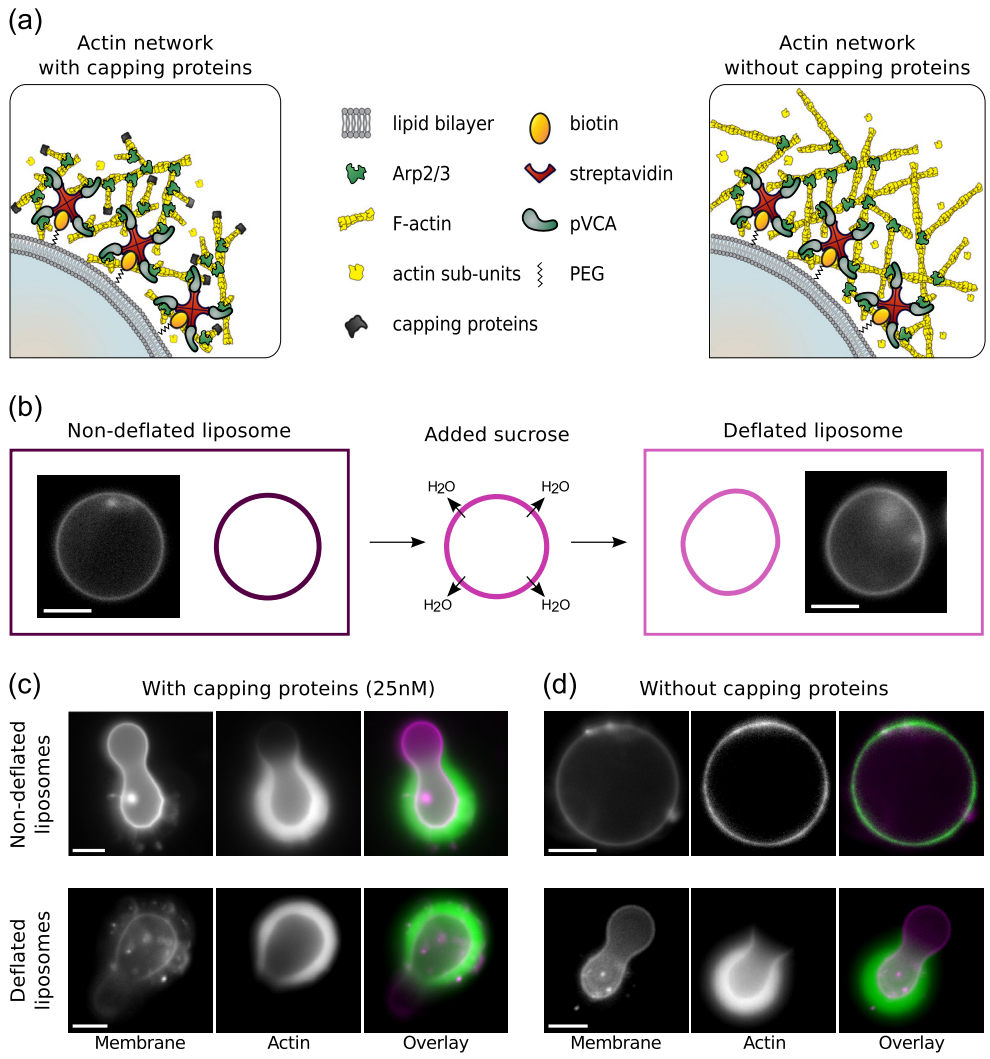

Figure 1. Experimental system. (a) Schemes of the purified proteins (legend) for the reconstitution of the branched actin network at the outer surface of liposomes (left, in the presence of CP, right, in the absence of CP); proteins not to scale. (b) Illustrative scheme of the method to obtain deflated liposomes (light purple, right) from non-deflated ones (dark purple, left) with corresponding examples of epifluorescence images of membrane (TexasRed-DHPE). (c) and (d) Epifluorescence images of representative examples of liposome deformations induced by actin polymerization in different conditions (indicated). Membrane (left, TexasRed DHPE), actin (middle, Alexa488-actin), and overlay (purple: membrane, green, actin). All scale bars, 5 μm.

a symmetry breaking event. Using this system, we now investigate how the occurrence of symmetry breaking depends on the presence of CP and membrane tension.

Role of capping proteins (CP) in actin-based symmetry breaking

To investigate the role of CP in actin-based symmetry breaking, we reconstitute an actin network in the absence of CP at the outer surface of liposomes (figure 1(a), right). The actin polymerization mixture thus contains only monomeric actin, profilin and the Arp2/3 complex, in the same conditions as previously used, with omission of CP. The absence of CP leads to a strong decrease in the occurrence of symmetry breaking of the actin network as we find that only 0.6% of liposomes display symmetry breaking in the absence of CP compared to 47.3% in the presence of CP (see above). Thin and homogeneous actin networks are indeed mainly observed (example in figure 1(d), top row). Thus, we conclude that capping proteins are essential to generate the symmetry breaking of the actin network, in line with what was observed with beads in the same spherical conditions [10].

Change of membrane tension in our system

To unveil the role of membrane tension in symmetry breaking of the actin network and how membrane shape changes, membrane tension of liposomes is decreased prior to actin polymerization (figure 1(b)). To do so, liposomes are first coated with the promotor of actin polymerization, SpVCA, and then deflated by incubation in a solution with higher osmolarity (400 mOsmol instead of 200 mOsmol). In fact, increasing the osmolarity of the outside solution creates an osmotic pressure difference, which equilibrates fast (within 30 min) with water leaving the inside of liposomes (scheme figure 1(b)) [25]. As a consequence, the apparent liposome volume decreases (images figure 1(b)), resulting in a decrease of membrane tension. While increasing the osmolarity of

the outside solution is necessary to deflate liposomes, it is important that all actin reagents are carefully at the same total concentration as in non-deflated conditions (Methods). Indeed, as an example, a decrease in ATP and salt concentration leads to a different percentage of symmetry breaking events in non-deflated conditions (figure S2).

Effect of liposome deflation on membrane shape and symmetry breaking, in the presence or absence of capping proteins

Liposome shapes are characterized by their form factor *e*, the ratio of the short and long radii of the best ellipse that fits their apparent contour on fluorescent membrane images (Methods). A form factor of 1 refers to a spherical liposome whereas a form factor closer to zero characterizes an elongated shape. We first observe liposomes only, i.e. in the absence of any actin dynamics. Non-deflated liposomes display a distribution of form factor close to 1 (figure 2(a), 83.0% of liposomes display a form factor between 0.95 and 1). As expected, deflated liposomes display a slightly broader distribution of form factors (figure 2(b), 66.0% of liposomes display a form factor between 0.95 and 1), and their contour fluctuates with time [26]. When the actin mix is present, liposome form factor measurement is complemented by the characterization of symmetry breaking (Methods). One striking result is that distributions of form factors are broader in the presence of an actin network than in its absence (figures 2(c), (d) and (f)), where respectively 54.7, 53.0, and 30.2% of liposomes display a form factor between 0.95 and 1), except when CP is absent and in non-deflated liposomes (figure 2(e), 91.7%).

Actin network symmetry breaking is observed more often for more deformed liposomes (green bars fill in purple bars of lower form factor, figure 2(c)). Strikingly, in the absence of CP and when liposomes are deflated, there is a huge increase of the occurrence of actin network symmetry breaking (figures 2(e) and (f)). In the presence of CP, the difference is less impressive, although there is more correlation of symmetry breaking with increased liposome deformation in deflated liposomes than in non-deflated ones (figures 2(c) and (d)). The more the liposomes are deformed (lower form factor), the more they display symmetry breaking (as seen by the coincidence of green and purple bars at lower form factor (figures 2(c), (d) and (f)). These results reveal that membrane tension, and the presence of CP, are key parameters to regulate the mechanical effects of actin dynamics, especially the ability of the network to break the symmetry and deform the membrane.

Discussion

Using a biomimetic system which allows to precisely control physical parameters, such as actin network detailed structure, or membrane tension, we find conditions that favor membrane deformations induced by actin polymerization. For that, we first confirm that liposome deformation is correlated with the asymmetry of the actin network, as the occurrence of symmetry breaking is mainly observed when liposomes have a lower form factor (figures 2(c), (d) and (f)).

In the presence of CP, filaments branch and elongate only at the surface of the liposomes, generating a perpendicular stress at the liposome surface and a tangential stress in the outer layer, which behaves as a dead zone of the network that builds up stress. This process can lead to symmetry breaking as described in the introduction [8, 9, 19]. This is the case in the concentrations we use here as a reference system for proper symmetry breaking to happen (37 nM Arp2/3 complex, 25 nM CP). In the absence of CP, a case that is less studied with liposomes, filaments elongate both at the liposome surface and at the outer layer of the actin shell. Therefore, the outer layer of the actin network is an active zone that grows and reforms constantly. As a consequence, we expect that the tangential stress of the outer layer is less pronounced than in the presence of CP. Consequently, in the absence of CP, symmetry breaking events are only rarely observed, as shown on beads [10], and on our liposome system (compare figures 2(c) and (e)). Note nevertheless that symmetry breaking was observed around beads at very high concentrations of the Arp2/3 complex, an indication that a stress could build up in the absence of CP [10]. The absence of symmetry breaking without CP in our system may therefore be attributed to an under-threshold of tangential stress in the outer layer whereas the orthogonal stress at the surface of the liposome should be unchanged. A way of revealing this possible remaining orthogonal stress at the surface of liposomes in the absence of CP is to decrease their membrane tension. This way, liposomes are expected to deform more easily if stresses buildup orthogonally to their membrane.

We find, indeed, that lowering membrane tension of liposomes in the absence of CP leads to a huge increase of symmetry breaking events and liposome deformations (compare figures 2(e) and (f)). This experiment proves that stresses are present at the liposome surface when CP is absent. They are revealed only when the membrane is deflated, as in these conditions, there is not enough opposing pressure to sustain these stresses (unlike when the membrane is non-deflated), and symmetry breaking occurs. In other words, decreasing membrane tension in liposomes resumes symmetry breaking and membrane deformations, and points to the importance of the interplay between membrane tension and network organization. Such parameters, especially membrane tension and liposome initial shape are not yet included in symmetry breaking theoretical models [6, 9, 27–29]. Based on our experiments, the process of symmetry breaking of the actin network may be theoretically addressed to unveil the role of tension, initial shape, and network

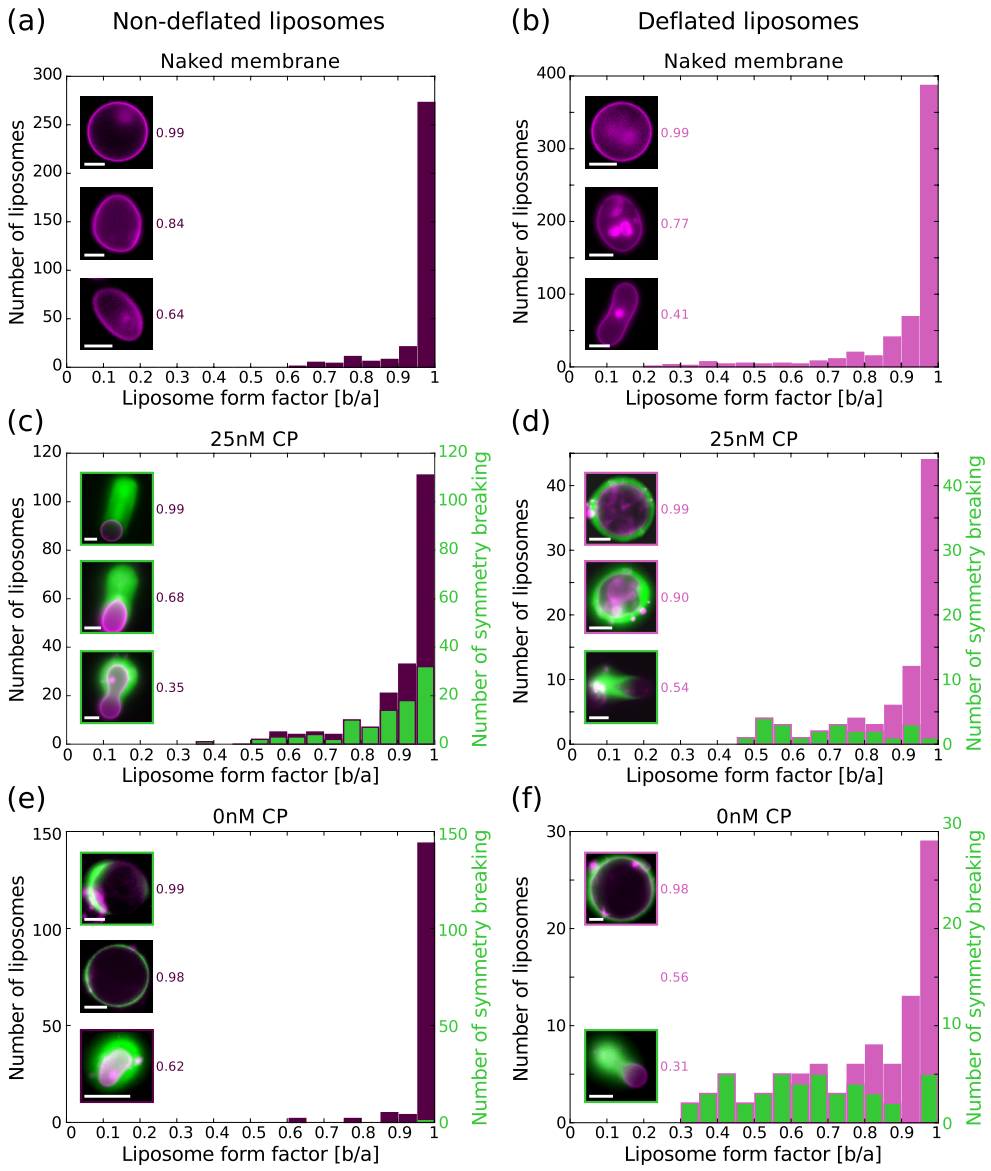

Figure 2. Membrane deformations and actin network symmetry breaking. Distribution of liposome form factors for non-deflated (dark purple bars) and deflated liposomes (light purple bars). (a) and (b) In the absence of actin ((a) $n = 329$ and (b) $n = 586$). (c)–(f) In the presence of actin with the additional count of actin symmetry breaking (green bars); note that green bars are always contained in the purple bars, as all liposomes of a population are characterized for form factor whereas only a portion of them display a symmetry breaking event. (c) and (d) At 25 nM CP for non-deflated ($n = 203$ from 3 experiments) and deflated liposomes ($n = 83$ from 2 experiments), respectively. (e) and (f) At 0 nM CP for non-deflated ($n = 157$ from 4 experiments) and deflated liposomes ($n = 96$ from 3 experiments), respectively. (a)–(f) Examples of epifluorescence images of membrane (purple, TexasRed DHPE) and actin network (green, Alexa488-actin) with indicated liposome form factor. Images surrounded by green boxes correspond to actin symmetry breaking whereas images surrounded by purple boxes do not show symmetry breaking of the actin network. All scale bars, 5 μm.

topology on the ability of a dynamics network to actually deform a membrane.

Interestingly, decreasing liposome tension in our reference conditions of protein concentrations in the presence of CP reveals the efficiency of actin dynamics to deform liposomes. This is observed by comparing figures 2(c) and (d) where the distribution of form factors is broader for deflated liposomes and symmetry breaking always matches lower form factors.

Membrane tension values of electroformed liposomes have been estimated previously in the same conditions as our non-deflated conditions, here, to 10^{-6} N $\cdot$ m^{-1} [30]. Given the typical radius of our liposomes, $R = 10$ μm, we can estimate the Laplace pressure to be $\Delta P = 10^{-1}$ Pa in non-deflated liposomes. The opposing pressure exerted by the actin network in the presence of CP is expected to be $p = E\left(\frac{h}{R}\right)^2$ where E is the Young modulus of the actin network, on the order of 10^4 Pa [8, 31], h the thickness of the actin network and R the radius of the spherical liposome. Taking $\frac{h}{R}$ on the order of 0.2 (see images), leads to an actin pressure on the order of $4 \cdot 10^2$ Pa, and represents an overestimate of the orthogonal pressure that may occur in the absence of CP. These estimates however reveal that the stresses exerted by the

actin network in the presence of CP are well over the Laplace pressure and that the liposome system is prone to deformation under the effect of the actin network. In the absence of CP, these deformations indicate the presence of stresses, and only appear when membrane tension is lowered and liposome shape able to change.

A careful examination of the effect of membrane tension and protein composition unveils here that cell shape changes may redundantly rely on both membrane tension and actin network details. This result is supported by recent results on endocytosis, where actin dynamics and membrane tension may play a crucial role on membrane deformation, a role that was previously attributed to coat proteins [2, 32, 33].

Conclusion

Our biomimetic system provides evidence that both the actin structure (presence of capping proteins) and membrane tension govern liposome shape changes induced by actin polymerization. When the actin structure lacks capping proteins, the sensitivity of the system to membrane tension is higher, and a decrease in membrane tension rescues membrane deformation in the absence of capping proteins. Theoretical approaches still need to be developed to unveil the mechanistic origin of this phenomenon. In cells, robustness is ensured by redundancy mechanisms, and may be illustrated by this observed sensitivity to membrane deformations by actin dynamics. *In vitro* systems are a powerful tool to dissect and quantify detailed mechanisms of shape changes, compared to the complexity of cellular systems.

Acknowledgments

We thank John Manzi for protein purification, and Julie Plastino for many fruitful discussions. This work was supported by the French Agence Nationale pour la Recherche (ANR), grant ANR-14-CE090006 and ANR-12-BSV5001401, and by the Fondation pour la Recherche Médicale (FRM), grant DEQ20120323737.

ORCID iDs

Camille Simon https://orcid.org/0000-0002-7060-5721
Clément Campillo https://orcid.org/0000-0003-4698-8643
Cécile Sykes https://orcid.org/0000-0003-3057-2600

References

[1] Small J V *et al* 2002 The lamellipodium: where motility begins *Trends Cell Biol.* **12** 112–20
[2] Kukulski W *et al* 2012 Plasma membrane reshaping during endocytosis is revealed by time-resolved electron tomography *Cell* **150** 508–20
[3] Blanchoin L *et al* 2014 Actin dynamics, architecture, and mechanics in cell motility *Physiol. Rev.* **94** 235–63
[4] Tilney L G and Portnoy D A 1989 Actin filaments and the growth, movement, and spread of the intracellular bacterial parasite, *Listeria monocytogenes J. Cell Biol.* **109** 1597–608
[5] Loisel T P *et al* 1999 Reconstitution of actin-based motility of Listeria and Shigella using pure proteins *Nature* **401** 613–6
[6] van Oudenaarden A and Theriot J A 1999 Cooperative symmetry-breaking by actin polymerization in a model for cell motility *Nat. Cell Biol.* **1** 493–9
[7] Bernheim-Groswasser A *et al* 2002 The dynamics of actin-based motility depend on surface parameters *Nature* **417** 308–11
[8] Noireaux V *et al* 2000 Growing an actin gel on spherical surfaces *Biophys. J.* **78** 1643–54
[9] van der Gucht J *et al* 2005 Stress release drives symmetry breaking for actin-based movement *Proc. Natl Acad. Sci. USA* **102** 7847–52
[10] Achard V *et al* 2010 A 'primer'-based mechanism underlies branched actin filament network formation and motility *Curr. Biol.* **20** 423–8
[11] Paluch E *et al* 2006 Deformations in actin comets from rocketing beads *Biophys. J.* **91** 3113–22
[12] Boukellal H *et al* 2004 Soft listeria: actin-based propulsion of liquid drops *Phys. Rev.* E **69** 3–6
[13] Giardini P A 2003 Compression forces generated by actin comet tails on lipid vesicles *Proc. Natl Acad. Sci. USA* **136** 1165–8
[14] Upadhyaya A *et al* 2003 Probing polymerization forces by using actin-propelled lipid vesicles *Proc. Natl Acad. Sci. USA* **100** 4521–6
[15] Plastino J and Sykes C 2005 The actin slingshot *Curr. Opin. Cell Biol.* **17** 62–6
[16] Trichet L *et al* 2007 VASP governs actin dynamics by modulating filament anchoring *Biophys. J.* **92** 1081–9
[17] Delatour V *et al* 2008 Arp2/3 controls the motile behavior of N-WASP-functionalized GUVs and modulates N-WASP surface distribution by mediating transient links with actin filaments *Biophys. J.* **94** 4890–905
[18] Heuvingh J, Franco M and Chavrier P 2007 ARF1-mediated actin polymerization produces movement of artificial vesicles *Proc. Natl. Acad. Sci. USA* **104** 16928–33
[19] Kawska A *et al* 2012 How actin network dynamics control the onset of actin-based motility *Proc. Natl Acad. Sci. USA* **109** 14440–5
[20] Palmgren S *et al* 2001 Interactions with PIP2, ADP-actin monomers, and capping protein regulate the activity and localization of yeast twinfilin *J. Cell Biol.* **155** 251–60
[21] Carvalho K *et al* 2013 Actin polymerization or myosin contraction: two ways to build up cortical tension for symmetry breaking *Phil. Trans. R. Soc. Lond.* B **368** 20130005
[22] Angelova M I and Dimitrov D S 1986 Liposome electroformation *Faraday Discuss. Chem. Soc.* **81** 303
[23] Lemière J, Carvalho K and Sykes C 2015 Cell-sized liposomes that mimic cell motility and the cell cortex *Methods Cell Biol.* **128** 271–85
[24] Theriot J A *et al* 1992 The rate of actin-based motility of intracellular Listeria monocytogenes equals the rate of actin polymerization *Nature* **357** 257–60
[25] Olbrich K *et al* 2000 Water permeability and mechanical strength of polyunsaturated lipid bilayers *Biophys. J.* **79** 321–7
[26] Sackmann E 1995 Physical basis of self-organization and function of membranes: physics of vesicles *Handbook of Biological Physics* vol 1 pp 213–304
[27] Sekimoto K *et al* 2004 Role of tensile stress in actin gels and a symmetry-breaking instability *Eur. Phys. J.* E **13** 247–59
[28] John K *et al* 2008 Nonlinear study of symmetry breaking in actin gels: implications for cellular motility *Phys. Rev. Lett.* **100** 2–5
[29] John K, Stöter T and Misbah C 2016 A variational approach to the growth dynamics of pre-stressed actin filament networks *J. Phys.: Condens. Matter* **28** 375101

[30] Caorsi V et al 2016 Cell-sized liposome doublets reveal active tension build-up driven by acto-myosin dynamics Soft Matter 12 6223–31
[31] Marcy Y et al 2004 Forces generated during actin-based propulsion: a direct measurement by micromanipulation Proc. Natl Acad. Sci. 101 5992–7
[32] Picco A et al 2018 The contributions of the actin machinery to endocytic membrane bending and vesicle formation Mol. Biol. Cell 29 1346–58
[33] Boulant S et al 2011 Actin dynamics counteract membrane tension during clathrin-mediated endocytosis Nat. Cell Biol. 13 1124–31